Construction and Building Materials 411 (2024) 134371

Contents lists available at ScienceDirect

Construction and Building Materials

journal homepage: www.elsevier.com/locate/conbuildmat

Effects of colloidal nanoSiO$_2$ on the hydration and hardening properties of limestone calcined clay cement (LC^3)

Mingqing Liu [a], Xiangming Zhou [a,*], Pengkun Hou [a], Ran Hai [b], Yuzhou Sun [b], Shuang Liang [a], Zhonghao Niu [a]

[a] Department of Civil and Environmental Engineering, Brunel University London, Uxbridge, Middlesex UB8 3PH, United Kingdom
[b] School of Architectural Engineering, Zhongyuan University of Technology, Zhengzhou 450007, China

ARTICLE INFO

Keywords:
Colloidal nanoSiO$_2$
Sulfation degree
Hydration
Mechanical property
Fluidity

ABSTRACT

This research investigates the influence of colloidal nanosilica (CNS) on the hydration and hardening properties of Limestone Calcined Clay Cement (LC^3). The sulfation degree for LC^3 was first optimized based on the hydration heat, and the results suggested that gypsum increases the cumulative heat release during the hydration process of LC^3, with a dosage of 2% by weight gypsum leading to the highest heat release. The effects of CNS on hydration reaction, fluidity, mechanical properties and microstructure of LC^3 were then investigated. According to the results obtained from isothermal calorimetry and thermogravimetric analysis, CNS can considerably accelerate the reaction rate of the LC^3 system. 3% and 5% by weight CNS can significantly improve the compressive strength of LC^3 blends, especially at early ages of 3 and 7 days. The findings from this study lead to a better understanding of the modification effects of CNS on LC^3 which subsequently provides an insight into regulation mechanism of CNS on LC^3.

1. Introduction

Portland cement has demonstrated its reliability in construction across a wide range of loading and service environments with a proven service history spanning over two centuries. Despite its comparatively low cost and low energy consumption compared to other construction materials, the large scale of its production worldwide results in anthropogenic CO_2 emissions accounting for 6–8% which mainly comes from the decarbonation of limestone during the clinkering process [1–5]. Consequently, dramatically reducing CO_2 emissions associated with cement production is the most critical and pressing challenge faced by the cement industry [6].

The use of supplementary cementitious materials (SCMs) to partially substitute clinker has a huge potential to reduce carbon emissions and also precious natural resource consumption in the cement industry [7]. So far, over 80% by weight of the SCMs that are adopted to reduce clinker in cement are ground granulated blast furnace slag (GGBS) and fly ash [8]. However, with the growing demand of using cleaner fuels in power plants, the supply of traditional SCMs (i.e., GGBS and fly ash) is expected to dramatically decrease in the near future [9]. Hence, it is crucial to broaden the range of low-carbon SCM resources, such as limestone and calcined clay, for cement production.

Limestone Calcined Clay Cement (LC^3) is a new type of cement that is based on a blend of clinker, limestone, calcined clay and gypsum [10]. The feasibility of LC^3 as an alternative to PC is attributed to the fact that kaolinitic clay and limestone, which are constitutive components of LC^3, are two widely distributed materials in many regions around the world [11]. Clays having a certain proportion of kaolinite have proven to be highly pozzolanic if calcined between 700 and 850 °C [12]. In LC^3, calcined clay reacts as pozzolanic material with portlandite, water and sulfate to form C-A-S-H, ettringite and AFm phases [13,14]. When limestone is added to cement, calcite reacts with C_3A from clinker and aluminate phase from calcined clay to form hemi- and mono-carboaluminate (Hc, Mc) phases [15–17]. The sequence of reactions can be described by the following Eqs. (1) - (4). This feature enables a greater substitution of clinker, resulting in a more refined and less interwoven microstructure that enhances the mechanical and durability performance of the LC^3 system [18].

$$Al_2O_3{\cdot}2SiO_2\ (AS_2)+Ca(OH)_2+H_2O\rightarrow C\text{-}(A)\text{-}S\text{-}H \quad (1)$$

$$AS_2+C_3A+CaSO_4{\cdot}2\ H_2O+H_2O\rightarrow 3CaO{\cdot}Al_2O_3{\cdot}3CaSO_4{\cdot}32\ H_2O\ (AFt) \quad (2)$$

* Corresponding author.
E-mail address: Xiangming.Zhou@brunel.ac.uk (X. Zhou).

https://doi.org/10.1016/j.conbuildmat.2023.134371
Received 18 September 2023; Received in revised form 8 November 2023; Accepted 27 November 2023
Available online 9 December 2023

$$AFt+AS_2+C_3A+H_2O \rightarrow 3CaO{\cdot}2Al_2O_3{\cdot}CaSO_4{\cdot}12\ H_2O\ (AFm) \quad (3)$$

$$AFm+CaCO_3+H_2O \rightarrow 4CaO{\cdot}2Al_2O_3{\cdot}(CO_3)_{0.5}{\cdot}(OH)_{12}{\cdot}12\ H_2O(Hc)/ 4CaO{\cdot}2Al_2O_3{\cdot}CO_3{\cdot}(OH)_{12}{\cdot}11\ H_2O\ (Mc) \quad (4)$$

It's important to note that the optimal sulfate level for LC^3 may vary compared to traditional Portland cement. In various studies, it has been noticed that LC^3 often necessitates extra gypsum in addition to achieve the highest compressive strength within 24 h [19,20]. Without sulfate adjustment, the aluminate peak may precede the alite peak, leading to a reduced and broader silicate peak. The introduction of additional gypsum shifts the aluminate peak to later stages and recovers the silicate peak.

Despite possessing numerous commendable advantages, LC^3 exhibits a lower early strength and slower strength gain in contrast to Portland cement [21]. Nano additives have been incorporated into cement and concrete to attain more robust and long-lasting concrete [22,23]. NanoSiO_2 (NS) is the most frequently utilized nanomaterial as an additive for cement and concrete, and has been extensively studied so far [24–27]. It has been widely documented that the inclusion of NS can significantly enhance the properties of cementitious materials [23–27]. Siang et al. [24] reported that 3% by weight NS can improve the compressive strength of mortar by 38% at 28 days; Meng et al. [25] found that NS can enhance the value and shorten the occurrence time of hydration exothermic peak of cement; Shih et al. [26] found that the ratio of maximum increase in compressive strength is about 60.6% at an age of 14 days and reduces to 43.8% at an age of 56 days with the addition of 0.6 wt% NS. This could be explained in three aspects. Firstly, due to its small particle size and high surface area, NS particles can fill the gaps between cement particles and improve the packing density of the paste. Secondly, the large surface area of NS particles allows for a higher degree of interaction with cement particles. Finally, NS particles can act as a nucleation agent for the formation of C-S-H gel which can lead to a denser microstructure and a reduction in porosity, resulting in improved mechanical properties such as strength and durability.

Currently, there is very limited research regarding the utilization of NS for regulating LC^3. This paper aims to improve the performance of LC^3 by NS. Sulfation degree adjustment in case of undersulfation, hydration acceleration mechanisms, mechanical properties, fluidity and hydration products were investigated, all of which help to provide a better understanding of the modification effects of NS on the LC^3 systems.

2. Materials and methods

2.1. Materials

The blended cement used in this paper was made from Portland cement (PC), quartz (Q) and three types of SCMs, i.e. metakaolin (MK), limestone (LS) and gypsum (Gyp). A type I Portland Cement (i.e. Grade 52.5) conforming to BS EN 197–1 was used in this study. The MK was purchased from BASF. The limestone was acquired from Scientific Laboratory Supplies with 98% purity. Gypsum (i.e. $CaSO_4{\cdot}2\ H_2O$) sourced from Sigma-Alrich (98 + grade) was used for the formulations. To facilitate NS homogeneously distributed in LC^3 paste, colloidal nanoSiO_2 (CNS), instead of NS powder, was used in the mixtures, which was obtained from Merck Life Science UK Limited with 50 wt% suspension in water. The sand used for making the mortars was graded river sand with 4 mm nominal maximum aggregate size. The quartz was made by grinding sand through a ball mill. It was used as an inert material together with metakaolin to simulate a calcined clay with 50% of calcined kaolinite. Polycarboxylic (PCE) based superplasticizer was used to achieve the same fluidity for all mortars. The chemical (by XRF) and phase (by XRD-Rietveld) compositions of the materials in the study are given in Table 1. The particle size distribution by laser diffraction, obtained after dispersing the powder in Isopropanol is presented in Fig. 1 which shows that the particle size of quartz is finer than metakaolin. The size difference between quartz may affect the contact and interaction between these materials, potentially reducing the overall pozzolanic activity and hindering the formation of additional C-S-H gel.

Table 1
Chemical (XRF) and phase compositions (XRD) of PC, metakaolin, quartz, limestone, and gypsum (*wt.*%).

	PC	Metakaolin	Quartz	Limestone	Gyp
CaO	63.83	0.03	-	54.78	32.48
SiO_2	18.92	51.83	99.7	0.18-	-
Al_2O_3	4.27	45.32	-	-	-
Fe_2O_3	3.58	2.95	-	0.02	-
SO_3	3.53	0.04	-	0.12	46.37
MgO	1.87	0.01	0.03	-	0.02
K_2O	0.86	0.42	0.17	0.13	0.01
Na_2O	0.21	-	-	-	0.01
TiO_2	0.29	1.02	-	-	-
LOI	1.48	1.21	0.1	43.04	20.91
C_3S	65.7	-	-	-	-
C_2S	4.9	-	-	-	-
C_3A	4.8	-	-	-	-
C_4AF	10.1	-	-	-	-
Gyp	6.4	-	-	-	-

2.2. Mixtures and preparation of samples

In this paper, LC^3 blends were made of 55% PC, 15% MK, 15% quartz, and 15% limestone all by weight. 15% MK and 15% quartz together were used to simulate 30% calcined clay with 50% calcined kaolinite content. The dosage of gypsum was optimized in the LC^3 system, as described in Section 3.1. For all blended pastes, CNS as an additive was added to the mixture but with different dosages, as specified in Table 2. Samples were prepared using a water-to-binder ratio of 0.5. Each sample was mixed for 2 min at 1600 rpm, and poured into the molds. The molds were put in the curing chamber and stripped off after one day. After specified days of standard curing (relative humidity (RH) $>$ 95%, 20 ℃), hydration of the pastes was stopped. To do so, all samples were immersed in pure isopropanol for 3 h, then moved to new pure isopropanol for another 24 h curing, and followed by being dried in a vacuum oven at 40 ℃ for 3 days. The dried hardened pastes were then stored in a vacuum chamber, ready for the thermogravimetric analysis (TGA), X-ray diffraction (XRD) and scanning electron microscopy (SEM) analyses.

2.3. Methods

2.3.1. Hydration heat

The heat release during hydration was measured in an isothermal calorimeter (TAM Air) for 72 h. 10 g of sample was poured in a glass ampoule, which was then sealed and put in the calorimeter.

2.3.2. Fluidity and compressive strength

For fluidity test, mortars were made with a binder-to-sand weight ratio of 1:3 as the mix propositions for binders are specified in Table 3. Fluidity of the samples was measured conforming to BS EN 12390–16:2019.

Regarding to mortar strength, superplasticizer was added to mortars to obtain similar fluidity. In accordance to BS EN 12390–16:2019, prismatic mortar samples of 4 cm × 4 cm× 16 cm were made and their compressive strength were measured at 3, 7, 28 days.

2.3.3. XRD

XRD tests (Bruker D8 Advance diffractometer) were carried out on freshly cut slices of hardened paste with voltage 40 mV and current 25 mA to assess the phase assemblage of the samples. The samples were crushed to a fine powder and pressed into a sample holder. The scanning program consisted in rotating between 5° and 70° 2θ with a step size of

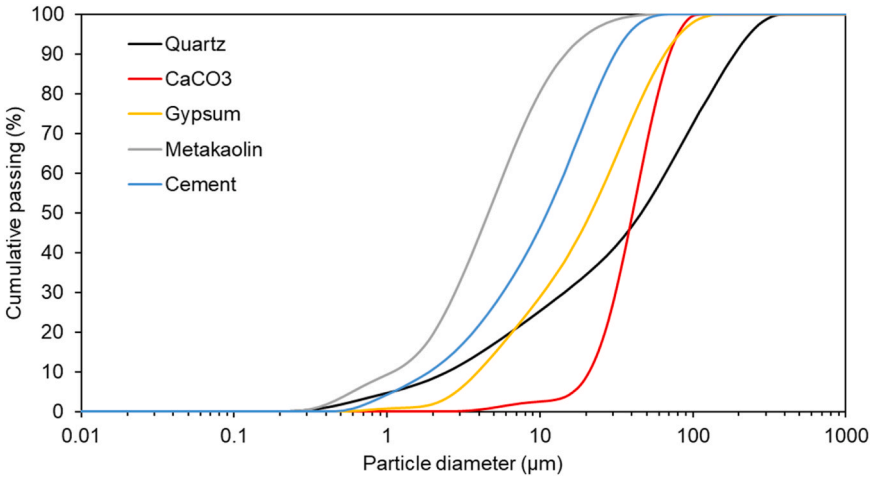

Fig. 1. Particle size distribution of the ingredients.

Table 2
Composition of mixes investigated (*wt.*%).

ID	PC	MK	Q	LS	Gyp	CNS	PCE (mortar)
LC^3-0 CNS	55	15	15	15	2	0	1.2
LC^3-1 CNS	55	15	15	15	2	1	1.5
LC^3-3 CNS	55	15	15	15	2	3	2.3
LC^3-5 CNS	55	15	15	15	2	5	3.0

Table 3
Mix proportions of LC^3 mixes (*wt.*%).

ID	PC	MK	Q	LS	Gyp
LC^3-0	55	15	15	15	0
LC^3-2	55	15	15	15	2
LC^3-3	55	15	15	15	3
LC^3-4	55	15	15	15	4

0.0167° 2θ.

2.3.4. SEM

Microscopic examinations of the hardened pastes were performed using an ultra-high-resolution scanning electron microscope (Supra 35VP, Carl Zeiss, Germany). Prior to the microscopic observations, the surfaces of the samples were coated with gold using an Edwards S150B sputter coater.

2.3.5. TGA

TGA of the pastes was performed using a simultaneous DSC/DTA/TGA system (C-Therm Technologies, New Brunswick, Canada). The heating rate was set at 10 °C/min, and the temperature range was between 30 and 950 °C.

3. Results and discussion

3.1. Sulfation degree adjustment

The main purpose of adding gypsum to LC^3 system is to achieve the desired reactivity balance between silicate phase and alumina phase. The mix compositions for sulfate adjustment of the LC^3 blends are shown in Table 3.

The rate of heat evolution regarding to the effect of gypsum on LC^3 is shown in Fig. 2. It can be seen that the silicate and aluminate peaks are separated by gypsum, and the aluminate peaks are depressed and delayed with the increase of gypsum dosage. Also, gypsum increases the cumulative heat release during cement hydration, and a dosage of 2% by weight results in the highest heat release.

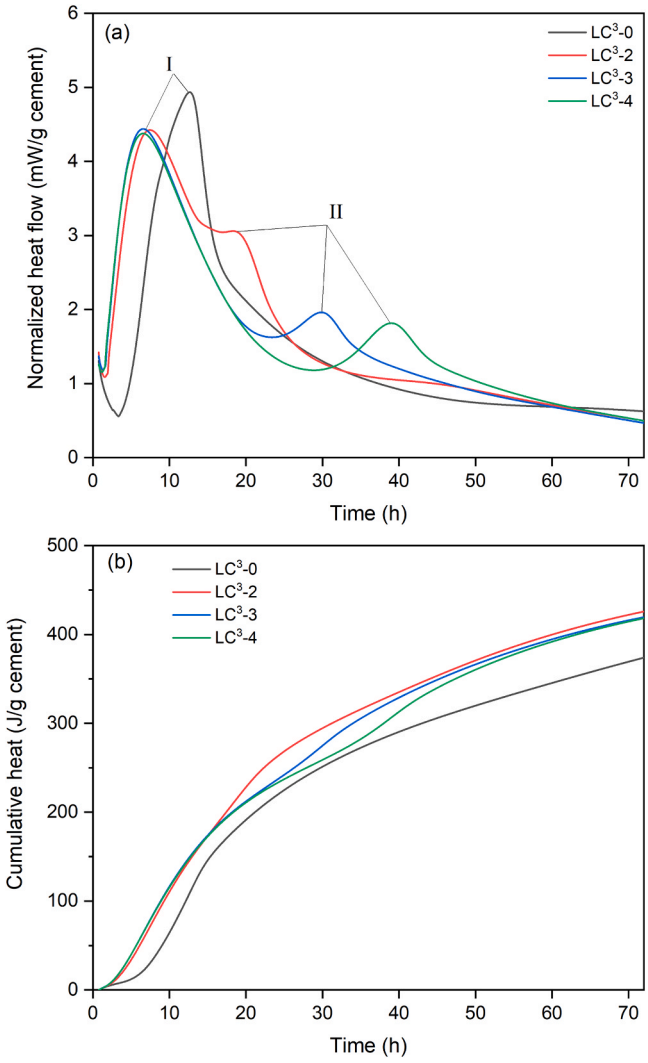

Fig. 2. (a) Normalized heat release per gram of cement and (b) cumulative heat released per gram of cement for LC^3 with different dosages of gypsum.

The onset of the acceleration stage was independent of the gypsum

content. The intensity of the silicate reaction peak (I) decreased slightly with increasing sulfate content, but this could be attributed to the separation of the overlapped aluminate peak (labeled as II). The peak labeled II, which is associated with the depletion of sulfate [28], showed the expected significant dependence on the sulfate content. It was retarded with the increasing sulfate content, with its maximum value being after 20, 30 and 40 h at 2%, 3% and 4% by weight gypsum contents, respectively. During the initial stages of hydration, the high concentration of sulfate in the pore solution is stabilized by the presence of calcium sulfates leading to sulfate adsorption on the C-S-H [29]. Once gypsum is depleted, the sulfate concentration in the pore solution drops with sulfates desorbing from the C-S-H. The continuing desorption of sulfate delays the sulfate depletion/aluminate reaction peak (II) [30].

3.2. Kinetics of hydration

The rate of heat evolution regarding to the effect of CNS on LC^3 is shown in Fig. 3. The incorporation of 1% and 3% both by weight CNS advanced and intensified the hydration peaks of silicate (i.e. the first peak). With the incorporation of small amount of CNS, the degree of hydration of cement is promoted, making the cement matrix produce more C-S-H gel, which can improve the pore structure of cement hydration. At the same time, a crystal nucleus is formed in the process of hydration and thus C-S-H can grow on its surface directly rather than adsorbed on the surface of unhydrated cement particles, thus affecting the speed and degree of hydration. However, the silicate peak was depressed by 5% by weight CNS. The depression of silicate reaction with the incorporation of a large amount of CNS may be due to a phenomenon called "particle packing effect" [31]. CNS particles have a very high specific surface area and tend to agglomerate, which can cause an increase in the viscosity of the cementitious system and hinder the movement of water molecules. As a result, the effective water-cement ratio may be reduced, leading to a decrease in the availability of water for cement hydration. In addition, the high surface area of CNS particles can lead to the formation of a thick gel-like layer around the cement particles, which can limit the diffusion of ions and delay the hydration process [32].

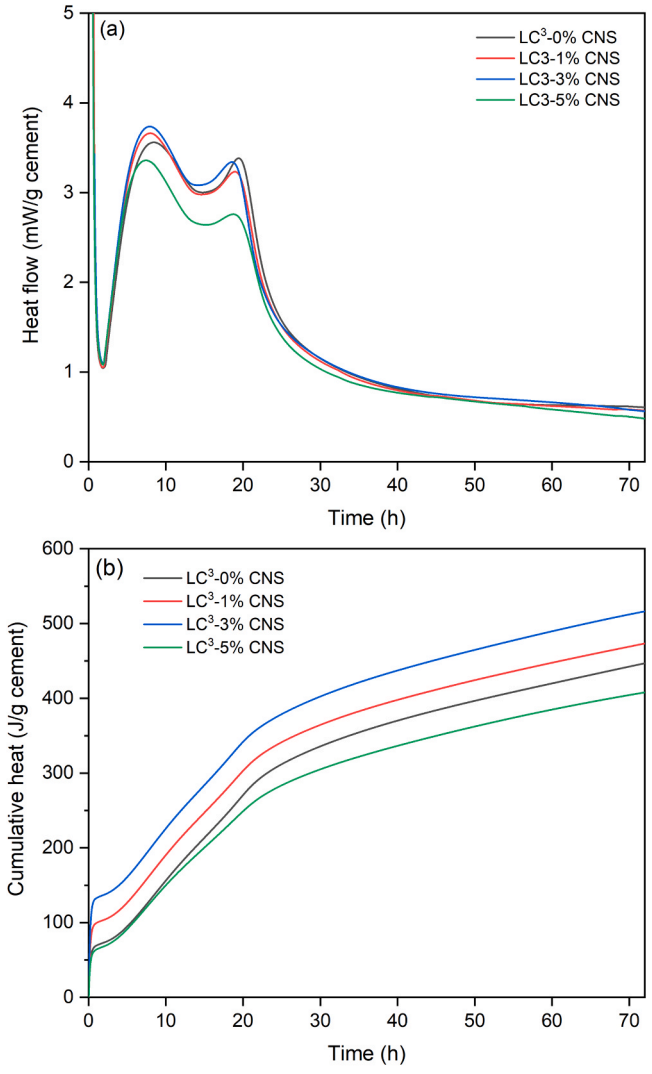

Fig. 3. Normalized heat release per gram of cement (a) and cumulative heat released per gram of cement (b) for LC^3 with different ratios of CNS.

It can also be found that the alumina peaks (i.e. the second peak) were depressed with the incorporation of CNS. The depression of the alumina reaction is possibly due to the consumption of aluminum ions in the formation of C-S-H gel [33]. CNS particles can react with the calcium hydroxide produced during cement hydration to form additional C-S-H gel, which requires the consumption of calcium and aluminum ions [34]. As a result, the available aluminum ions for the formation of aluminum hydrate phases such as C_3AH_6 (tricalcium aluminate hydrate) is reduced, leading to a depression of the alumina peak [35]. Additionally, the presence of CNS can modify the microstructure of the cementitious system, leading to changes in the distribution and availability of aluminum ions, which may also contribute to the depression of the alumina peak [36].

3.3. Workability and compressive strength

The fluidity of fresh LC^3 mortars with different ratios of CNS is shown in Table 4. With the incorporation of CNS, the fluidity of LC^3 mixture is greatly decreased. The addition of CNS to LC^3 reduces its workability due to its high surface area and small particle size. Nano-silica particles tend to agglomerate and form clusters, which can cause a reduction in the mobility of cement particles, resulting in a decrease in workability [37]. Additionally, the surface charge of nano particles can interact with that of cement particles, resulting in the formation of electrostatic bonds. These bonds can lead to a decrease in the dispersion of the cement particles and, therefore, cause the cement to become more viscous, further reducing its workability [38]. Furthermore, the addition of CNS can cause the cement to set more rapidly, leading to a shorter working time and making it difficult to place and finish. This is due to the fact that the high surface area and small particle size of nano-silica can accelerate the hydration process of the cement, leading to an earlier onset of the setting time [39].

The compressive strength of LC^3 composite with four dosages of CNS at four ages is presented in Fig. 4. Furthermore, Table 5 illustrates the enhanced compressive strength observed form LC^3 blends with various dosages if CNS compared to the control group. Basically, the compressive strength at four different stages exhibited a positive correlation with the amount of CNS present, especially at early ages. Notably, the incorporation of 5% by weight CNS yielded the most substantial increase in compressive strength across all ages, with a rise of 31% after 3 days and 26% after 7 days. Nevertheless, in the later ages, the increase rate decreases. The enhanced compressive strength of hardened LC^3 resulting from the addition of CNS can be attributed to at least two plausible mechanisms. Firstly, the small CNS particles can penetrate the pore structure of the material and fill the voids, thereby reducing porosity and increasing the material's density and strength. Secondly, the CNS particles can react with the calcium hydroxide, producing additional

Table 4
Fluidity of mortars with different dosages of CNS.

ID	LC3-0CNS	LC3-1CNS	LC3-3CNS	LC3-5CNS
f(mm)	170	160	110	90

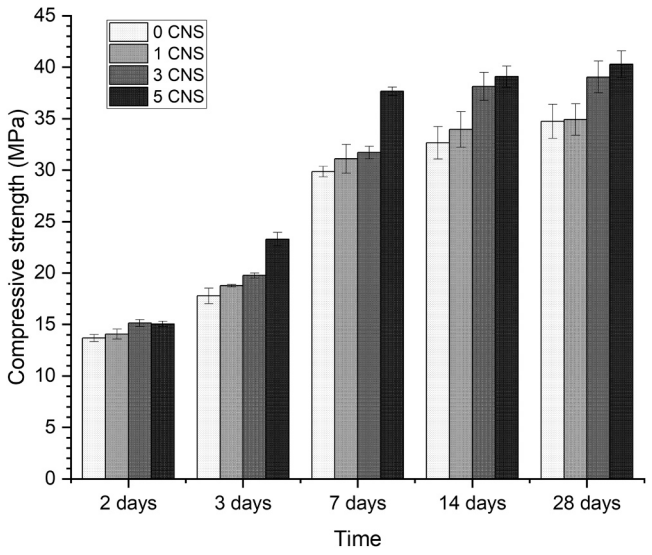

Fig. 4. Influence of CNS content (0%, 1%, 3% and 5%) on the compressive strength evolution of LC^3.

Table 5
Increase of compressive strength of samples with various dosages of CNS compared to the control group.

ID	3 days	7 days	14 days	28 days
1 CNS	5.6%	4.2%	4.0%	0.5%
3 CNS	11.1%	6.2%	16.8%	12.4%
5 CNS	31.0%	26.2%	19.8%	16.0%

calcium silicate hydrate (C-S-H) gel. This reaction leads to a denser matrix and an increase in strength. In addition, CNS reacts rapidly with calcium hydroxide to form calcium silicate in an alkaline environment such as the pore solution of LC^3 paste. Thus, the contribution of added CNS to the increase in strength of the hardened LC^3 blend becomes apparent in the early days of hydration.

When comparing the impact of CNS on the mechanical properties of cement, Hou et al. [40] reported that a 5% by weight addition of CNS can enhance the compressive strength of CEM 1 mortar by 45% at 7 days and 12% at 28 days. The influence of CNS on the strength development of LC3 is less pronounced than that of CEM 1 at early ages (7 days), but becomes more significant at later ages (28 days). This difference can be attributed to the increased involvement of cement hydration due to the nucleation effect of nanoparticles during the early stages. However, as time progresses, a higher degree of metakaolin participates in the hydration process.

3.4. Hydration products

XRD patterns at 1, 3 and 28 days of hydrated LC^3 blends with various dosages of CNS are shown in Fig. 5. After 1 day of hydration, as shown in Fig. 5(a), the ettringite and Mc peaks were observed at different diffraction angles. It can be seen that the intensity of portlandite (CH) was decreased with the increase of CNS. Mc has a three-dimensional structure with positively charged calcium, aluminum, and hydroxide ions surrounded by negatively charged carbonate ions [41]. It contributes to the long-term strength of cement and can also help to improve its durability. Consumption of CH can be considered as the pozzolanic activity of CNS that consumed part of portlandite.

At 3 days, with the process of hydration, Hc were observed. It contributes to the early strength of cement and can also help to stabilize the pH of the cement paste. Numerous studies have shown that carboaluminate hydrate can increase strength by filling the pore spaces [42,43].

At 28 days, portlandite was almost depleted as the result of the progression of hydration. The amounts of hydration products like ettringite, Hc and Mc were basically at the same level in all pastes though with different dosages of CNS. The hydration degree cannot be deduced from the change of amorphous phase content, but the variation of portlandite can be a good indicator of the hydration degree. The Portlandite content in the LC^3 paste with CNS was lower than in the control group, confirming that the calcined clay consumed CH to generate additional amorphous C-A-S-H gel.

3.5. Microstructure morphology

After curing for 28 days, the samples of LC^3-0CNS and LC^3-3CNS, containing 0% and 3%, respectively, by weight colloidal nanosilica, were observed by SEM, as depicted in Fig. 6. The SEM images revealed that the samples of LC^3-0CNS possessed many pores and a relatively loose structure with many pores, whereas the microstructure of LC^3-3CNS was denser and contained fewer pores. These observations suggest that the filler effect of nano silica and its pozzolanic activity contribute to increasing the density of the matrix. NS addition increased the quantity of C-(A)-S-H [44] in the cement paste and make the microstructure more compact [45,46]. Consequently, the addition of nano silica can increase the compressive strength of LC^3 blend pastes, which can be supported by the results of compressive strength with CNS which shows an increased effect on LC^3 blends.

3.6. Thermogravimetric analysis

3.6.1. Calcium hydroxide (CH) content

The weight loss observed between 450 °C and 550 °C was considered to be the decomposition of CH. The CH content, determined by TGA, is shown in Fig. 7 for LC^3 with varying ratios of CNS at both 3 and 28 days. At 3 days, the CH content decreased in the samples with the addition of CNS especially with 3% and 5% both by weight CNS. At 28 days, there is no big difference in CH content between the control group and the CNS-added group. In addition, the CH content greatly decreased with progress of hydration.

NS, a pozzolanic material, can react with calcium hydroxide to form additional C-(A)-S-H, thereby reducing the amount of CH in the system. This reaction consumes calcium hydroxide and produces more stable calcium silicate hydrates (C-S-H), which can improve the strength and durability of the cementitious material. Besides, the pozzolanic reaction of metakaolin can result in the formation of more C-(A)-S-H gel, which consumes CH during its formation, leading to a decrease in the overall content of CH in the final product. Furthermore, high concentrations of NS can act as nucleation sites for the precipitation of CH [47], resulting in an increase in its content.

3.6.2. Bound water (BW) content

The weight loss observed between 40 °C and 550 °C was attributed to the decomposition of BW. Monitoring the change of the amount of BW is one of the most commonly used methods for monitoring cement hydration. When compared 3 days and 28 days weight loss of BW in Fig. 8, it can be seen that the BW content increased with the progression of hydration. Additionally, there was no much difference in the BW content in samples with different dosages of CNS at 3 days. However, the BW content increased as the amount of CNS increased. NS particles, due to its pozzolanic activity, reacts with CH produced during cement hydration to form additional C-S-H gel. This reaction consumes water and contributes to the increased formation of hydration products, including BW. The additional C-S-H gel formed with the incorporation of CNS requires more water for its formation, resulting in an overall increase in the amount of BW in the LC^3 paste [40].

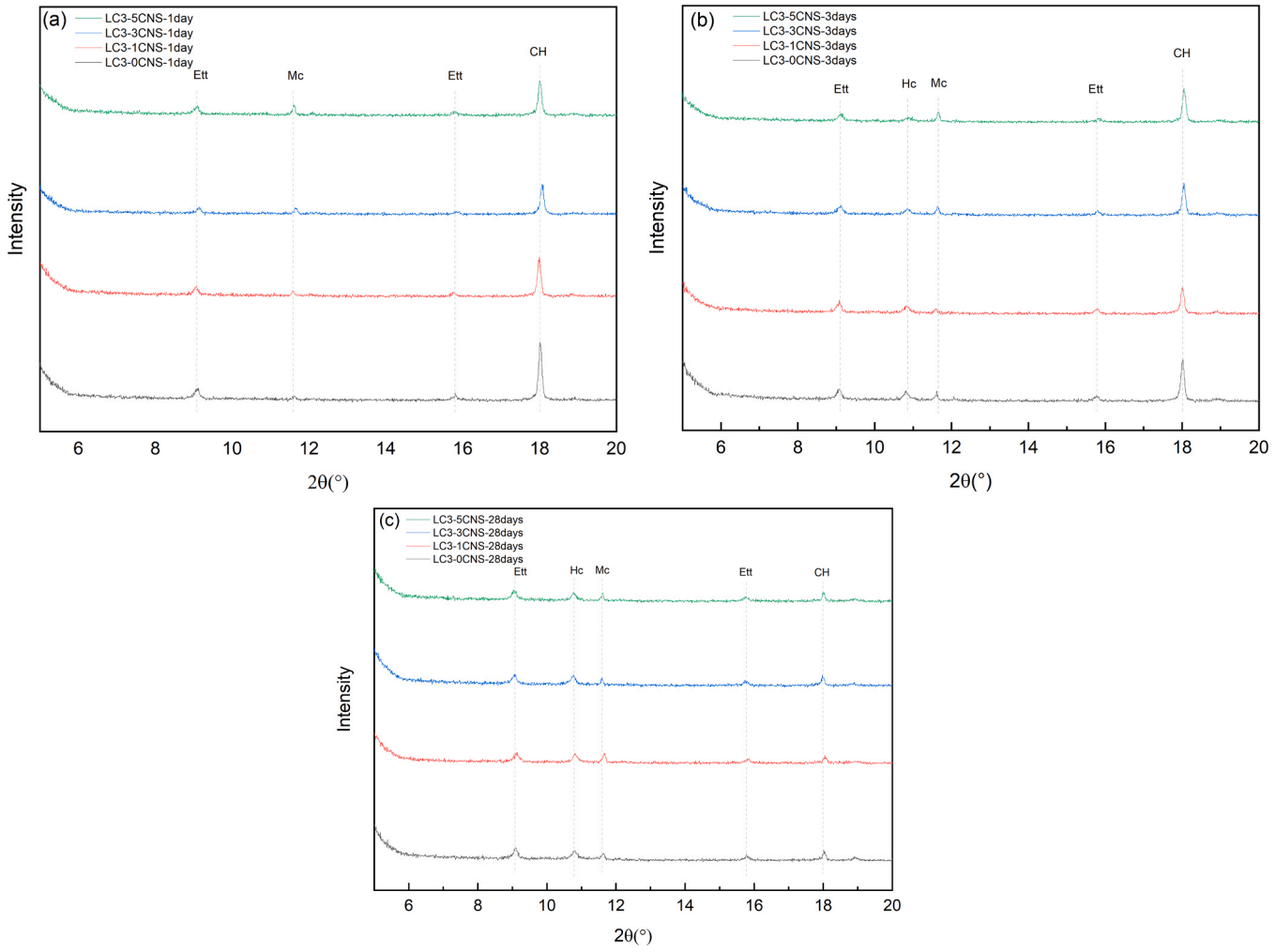

Fig. 5. XRD patterns of LC^3 pastes at 1 day (a), 3days (b) and 28 days (c) (Ett: ettringite, Hc: hemicarboaluminate, Mc: monocarboaluminate, CH: portlandite).

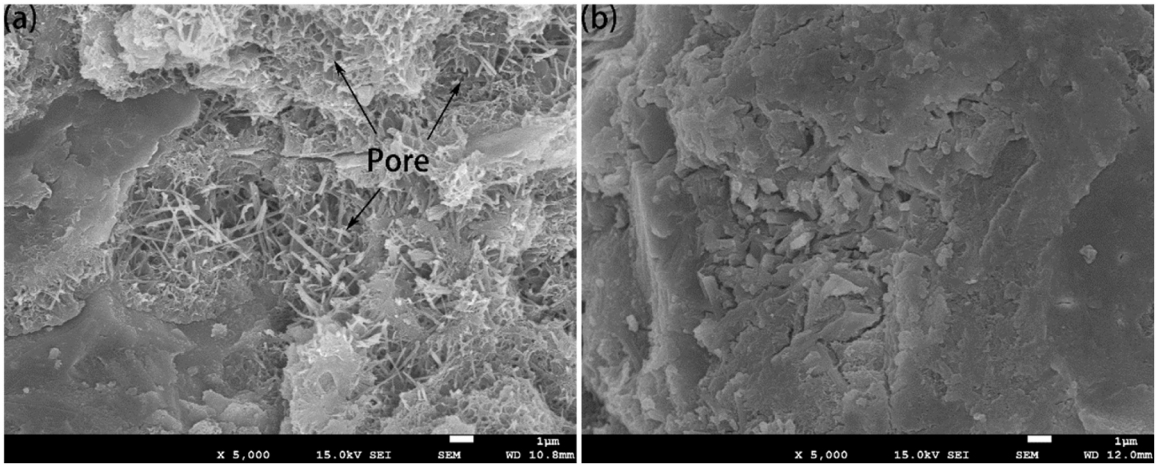

Fig. 6. SEM images of (a) LC^3-0CNS and (b) LC^3-3CNS with a magnification of 5000.

4. Conclusions

The LC^3, containing around only 50% clinker, is a new type of promising low-carbon energy-saving cement, however, the lower early strength has been a fatal factor limiting its wider applications in construction. In this study, CNS was added into the LC^3 system, aiming at promoting its development of mechanical property. Based on the results and analysis presented in this paper, the following conclusions can be drawn:

(1) Gypsum adjustment and reaction control: Gypsum is added to adjust the sulfation degree of LC^3, preventing flash setting by

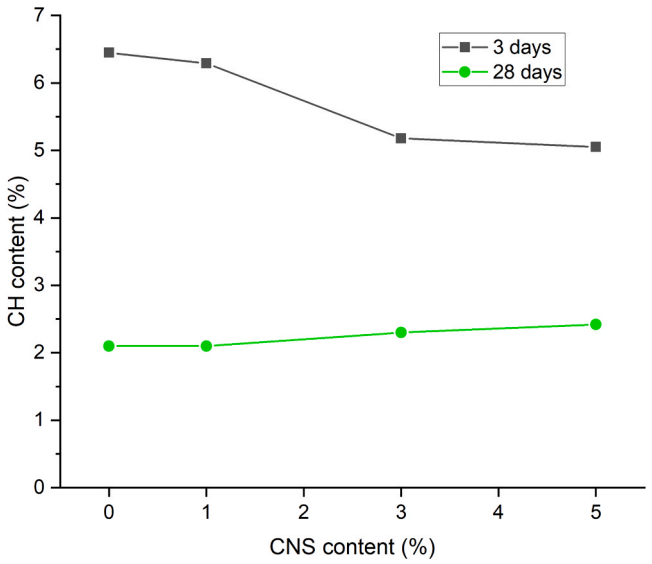

Fig. 7. Effect of CNS on CH content of LC^3 paste.

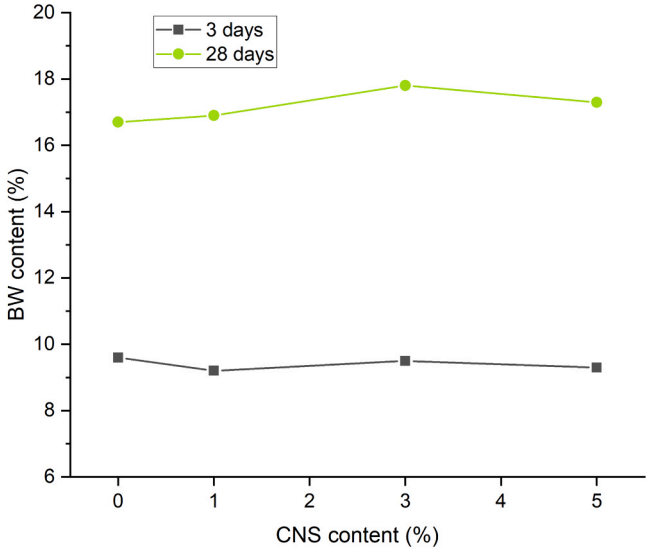

Fig. 8. Effect of CNS on BW content of LC^3 paste.

controlling the reaction of alumina. The optimal dosage of gypsum is found to be 2% by weight, which balances the silicate and alumina reactions in the LC^3 system.

(2) Influence of CNS addition: Isothermal calorimetry results reveal that the addition of 1% and 3% both by weight CNS advances and intensifies silicate peaks, while the addition of 5% by weight CNS depresses the silicate peak. Alumina peaks are also depressed due to the consumption of aluminum ions during the formation of C-S-H gel. Incorporating CNS decreases the workability of the LC^3 blend due to its high surface area and small particle size.

(3) Compressive strength and hydration products: The addition of 5% by weight CNS significantly increases compressive strength of LC^3 system, particularly at early ages, with a 31% rise at 3 days and a 26% rise at 7 days observed. XRD analysis shows that CNS accelerates the formation of hydration products, increasing the amount of Mc and decreasing the amount of portlandite. SEM images reveal that the microstructure of LC^3 paste becomes denser with the addition of CNS. TGA results confirm a decrease in CH (calcium hydroxide) content with CNS incorporation, which aligns well with the findings of XRD.

This study presents the application of CNS on the hydration and hardened properties of LC^3 system. In future research, it will be essential to evaluate the impact of CNS on the hydration degree of LC^3, considering both clinker and calcined clay components. Additionally, a comprehensive examination of the influence of CNS on the hardening and hardened properties of LC^3 with varying qualities of calcined clay should be conducted.

CRediT authorship contribution statement

Hai Ran: Writing – review & editing. **Hou Pengkun:** Writing – review & editing, Conceptualization. **Zhou Xiangming:** Writing – review & editing, Supervision. **Liu Mingqing:** Writing – original draft, Formal analysis. **Niu Zhonghao:** Data curation. **Liang Shuang:** Writing – review & editing. **Sun Yuzhou:** Writing – review & editing.

Declaration of Competing Interest

The authors declare that they have no known competing financial interests or personal relationships that could have appeared to influence the work reported in this paper.

Data availability

The data that has been used is confidential.

Acknowledgment

The first author would like to acknowledge Zhongyuan University of Technology for providing the partial PhD studentship for him for conducting this research at Brunel University London. The authors would like to acknowledge the Engineering and Physical Science Research Council for sponsoring this research through the grant EP/X04145X/1. This project has also received funding from the European Union's Horizon 2020 Research and Innovation Program under the Marie Skłodowska-Curie grant agreement No [893469].

References

[1] J. Yu, D.K. Mishra, C. Hu, C.K.Y. Leung, S.P. Shah, Mechanical, environmental and economic performance of sustainable grade 45 concrete with ultrahigh-volume limestone-calcined clay (LCC), Resour., Conserv. Recycl. 175 (2021), 105846.
[2] J. Li, G. Geng, W. Zhang, Y. Yu, D.A. Shapiro, P.J.M. Monteiro, The hydration of β- And α′ H -dicalcium silicates: an X-ray spectromicroscopic study, ACS Sustain. Chem. Eng. 7 (2) (2019) 2316–2326.
[3] R.G. Pillai, R. Gettu, M. Santhanam, S. Rengaraju, Y. Dhandapani, S. Rathnarajan, A.S. Basavaraj, Service life and life cycle assessment of reinforced concrete systems with limestone calcined clay cement (LC^3), Cem. Concr. Res. 118 (2019) 111–119.
[4] L. Wang, L. Chen, D.W. Cho, D.C.W. Tsang, J. Yang, D. Hou, K. Baek, H.W. Kua, C. S. Poon, Novel synergy of Si-rich minerals and reactive MgO for stabilisation/solidification of contaminated sediment, J. Hazard. Mater. 365 (2019) 695–706.
[5] L. Wang, L. Chen, J.L. Provis, D.C.W. Tsang, C.S. Poon, Accelerated carbonation of reactive MgO and Portland cement blends under flowing CO_2 gas, Cem. Concr. Compos. 106 (2020), 103489.
[6] S.A. Miller, G. Habert, R.J. Myers, J.T. Harvey, Achieving net zero greenhouse gas emissions in the cement industry via value chain mitigation strategies, One earth (Camb., Mass.) 4 (10) (2021) 1398–1411.
[7] R. Snellings, P. Suraneni, J. Skibsted, Future and emerging supplementary cementitious materials, Cem. Concr. Res. 171 (2023).
[8] WBCSD, Cement Sustainability Initiative. Getting the numbers right. ⟨http://www.wbcsdcement.org/index.php/key-issues/climate-protection/gnr-database⟩.
[9] G. Xu, X. Shi, Characteristics and applications of fly ash as a sustainable construction material: a state-of-the-art review, Resour., Conserv. Recycl. 136 (2018) 95–109.
[10] K. Scrivener, A. Favier (Eds.), Calcined Clays for Sustainable Concrete, RILEM Bookseries 10, Springer, 2015.
[11] Y. Cao, Y. Wang, Z. Zhang, Y. Ma, H. Wang, Recent progress of utilization of activated kaolinitic clay in cementitious construction materials, Compos. Part B, Eng. 211 (2021), 108636.
[12] R. Fernandez, F. Martirena, K.L. Scrivener, The origin of the pozzolanic activity of calcined clay minerals: a comparison between kaolinite, illite and montmorillonite, Cem. Concr. Res 41 (1) (2011) 113–122.

[13] A.S. Silva, A. Gameiro, J. Grilo, R. Veiga, A. Velosa, Long-term behavior of lime–metakaolin pastes at ambient temperature and humid curing condition, Appl. Clay Sci. 88–89 (2014) 49–55.
[14] A. Tironi, M.A. Trezza, A.N. Scian, E.F. Irassar, Assessment of pozzolanic activity of different calcined clays, Cem. Concr. Compos. 37 (2013) 319–327.
[15] B. Lothenbach, G. Le Saout, E. Gallucci, K. Scrivener, Influence of limestone on the hydration of Portland cements, Cem. Concr. Res. 38 (2008) 848–860.
[16] V.L. Bonavetti, V.F. Rahhal, E.F. Irassar, Studies on thecarboaluminate formation in limestone filler-blended cements, Cem. Concr. Res. 31 (2001) 853–859.
[17] M. Antoni, J. Rossen, F. Martirena, K. Scrivener, Cement substitution by a combination of metakaolin and limestone, Cem. Concr. Res 42 (2012) 1579–1589.
[18] Y. Dhandapani, T. Sakthivel, M. Santhanam, R. Gettu, R.G. Pillai, Mechanical properties and durability performance of concretes with limestone calcined clay cement (LC^3), Cem. Concr. Res. 107 (2018) 136–151.
[19] Z. Shi, S. Ferreiro, B. Lothenbach, M.R. Geiker, W. Kunther, J. Kaufmann, et al., Sulfate resistance of calcined clay – Limestone – Portland cements, Cem. Concr. Res. 116 (2019) 238–251.
[20] R. Hay, L. Li, K. Celik, Shrinkage, hydration, and strength development of limestone calcined clay cement (LC^3) with different sulfation levels, Cem. Concr. Compos. 127 (2022), 104403.
[21] K. Scrivener, F. Martirena, S. Bishnoi, S. Maity, Calcined clay limestone cements (LC^3), Cem. Concr. Res. 114 (2018) 49–56.
[22] Sobolev K., Shah S.P. Nanotechnology of concrete: recent developments and future perspectives. ACI Mater J 2008 [special publication].
[23] Collepardi M., Collepardi S., Skarp U., et al. Optimization of silica fume, fly ash and amorphous nano-silica in superplasticized high-performance concretes. In: Proceedings of 8th CANMET/ACI international conference on fly ash, silica fume, slag and natural pozzolan in concrete SP221 USA, vol. 30; 2004. p. 495–506.
[24] Ng.D. Siang, S.C. Paul, V. Anggraini, S.Y. Kong, T.S. Qureshi, C.R. Rodriguez, et al., Influence of SiO_2, TiO_2 and Fe_2O_3 nanoparticles on the properties of fly ash blended cement mortars, Constr. Build. Mater. 258 (2020), 119627.
[25] T. Meng, Y. Hong, H. Wei, Q. Xu, Effect of nano-SiO_2 with different particle size on the hydration kinetics of cement, Thermochim. Acta 675 (2019) 127–133.
[26] J.Y. Shih, T.P. Chang, T.C. Hsiao, Effect of nanosilica on characterization of Portland cement composite, Mater. Sci. Eng. A 424 (2006) 266–274.
[27] A.M. Said, M.S. Zeidan, Enhancing the reactivity of normal and fly ash concrete using colloidal nano-silica, Acids Mater. J. 267 (2009) 75–86.
[28] Andrade Neto, José da Silva, De. la Torre, G. Angeles, A.P. Kirchheim, Effects of sulfates on the hydration of Portland cement – a review, Constr. Build. Mater. 279 (2021), 122428.
[29] S. Pourchet, L. Regnaud, J.P. Perez, A. Nonat, Early C_3A hydration in the presence of different kinds of calcium sulfate, Cem. Concr. Res. 39 (11) (2009) 989–996.
[30] S. Mohammed, O. Safiullah, Optimization of the SO_3 content of an Algerian Portland cement: study on the effect of various amounts of gypsum on cement properties, Constr. Build. Mater. 164 (2018) 362–370.
[31] K. Nandhini, V. Ponmalar, Investigation on nano-silica blended cementitious systems on the workability and durability performance of self-compacting concrete, Mater. Express 10 (1) (2020) 10–20.
[32] D. Zheng, M. Monasterio, W. Feng, W. Tang, H. Cui, Z. Dong, Hydration characteristics of tricalcium aluminate in the presence of nano-silica, Nanomaterials 11 (1) (2021) 1–11.
[33] P. Dong, A. Allahverdi, C.M. Andrei, N.D. Bassim, The effects of nano-silica on early-age hydration reactions of nano Portland cement, Cem. Concr. Compos. 133 (2022), 104698.
[34] S. Papatzani, Effect of nanosilica and montmorillonite nanoclay particles on cement hydration and microstructure, Mater. Sci. Technol. 32 (2) (2016) 138–153.
[35] H.M. Son, S.M. Park, J.G. Jang, H.K. Lee, Effect of nano-silica on hydration and conversion of calcium aluminate cement, Constr. Build. Mater. 169 (2018) 819–825.
[36] R.H. Faraj, A.A. Mohammed, K.M. Omer, Microstructure characteristics, stress–strain behaviour, fresh properties, and mechanical performance of recycled plastic aggregate self-compacting concrete modified with nano-silica, Constr. Build. Mater. 383 (2023), 131371.
[37] M.P. Gashti, S. Moradian, A. Rashidi, M. Yazdanshenas, Dispersibility of hydrophilic and hydrophobic nano-silica particles in polyethylene terephthalate films: evaluation of morphology and thermal properties, Polym. Polym. Compos. 23 (5) (2015) 285–296.
[38] M. Berra, F. Carassiti, T. Mangialardi, A.E. Paolini, M. Sebastiani, Effects of nanosilica addition on workability and compressive strength of Portland cement pastes, Constr. Build. Mater. 35 (2012) 666–675.
[39] M. Zhang, J. Islam, Use of nano-silica to reduce setting time and increase early strength of concretes with high volumes of fly ash or slag, Constr. Build. Mater. 29 (1) (2012) 573–580.
[40] P. Hou, S. Kawashima, D. Kong, D.J. Corr, J. Qian, S.P. Shah, Modification effects of colloidal nanoSiO_2 on cement hydration and its gel property, Compos. Part B, Eng. 45 (1) (2013) 440–448.
[41] L.G. Baquerizo, T. Matschei, K.L. Scrivener, M. Saeidpour, L. Wadsö, Hydration states of AFm cement phases, Cem. Concr. Res. 73 (2015) 143–157.
[42] S. Krishnan, S. Bishnoi, Understanding the hydration of dolomite in cementitious systems with reactive aluminosilicates such as calcined clay, Cem. Concr. Res 108 (2018) 116–128.
[43] Y. Dhandapani, M. Santhanam, G. Kaladharan, S. Ramanathan, Towards ternary binders involving limestone additions — a review, Cem. Concr. Res. 143 (2021), 106396.
[44] J.I. Tobón, J.J. Payá, M.V. Borrachero, O.J. Restrepo, Mineralogical evolution of Portland cement blended with silica nanoparticles and its effect on mechanical strength, Constr. Build. Mater. 36 (2012) 736–742.
[45] B. Jo, C. Kim, J. Lim, Characteristics of cement mortar with nano-SiO_2 particles, Acids Mater. J. 104 (4) (2007) 404–407.
[46] F. Kontoleontos, P.E. Tsakiridis, A. Marinos, V. Kaloidas, M. Katsioti, Influence of colloidal nanosilica on ultrafine cement hydration: physicochemical and microstructural characterization, Constr. Build. Mater. 35 (2012) 347–360.
[47] D. Kong, S. Huang, D. Corr, Y. Yang, S.P. Shah, Whether do nano-particles act as nucleation sites for C-S-H gel growth during cement hydration? Cem. Concr. Compos. 87 (2018) 98–109.